

LETTER • OPEN ACCESS

Satellite detected weak decline of nitrogen oxides emissions in economically small cities of China

To cite this article: Hao Kong *et al* 2025 *Environ. Res. Lett.* **20** 074046

View the [article online](#) for updates and enhancements.

You may also like

- [Observation of intermediate template directed SiC nanowire growth in Si-C-N systems](#)
Min Xia, Shize Yang, Hongyan Guo et al.
- [Probing the vector charge of Sagittarius A* with pulsar timing](#)
Zexin Hu, Lijing Shao, Rui Xu et al.
- [Research on Advanced Driver Assistance System Oriented Height Distortion Hierarchical Shape Point Matching and Interpolation Algorithm](#)
Kai Zhang and Weili Wang

UNITED THROUGH SCIENCE & TECHNOLOGY



The Electrochemical Society
Advancing solid state & electrochemical science & technology

248th ECS Meeting

Chicago, IL
October 12-16, 2025
Hilton Chicago



**Science +
Technology +
YOU!**

Register by
September 22
to **save \$\$**

REGISTER NOW

ENVIRONMENTAL RESEARCH
LETTERS

LETTER

Satellite detected weak decline of nitrogen oxides emissions in economically small cities of China

OPEN ACCESS

RECEIVED

14 March 2025

REVISED

20 May 2025

ACCEPTED FOR PUBLICATION

5 June 2025

PUBLISHED

16 June 2025

Original content from this work may be used under the terms of the [Creative Commons Attribution 4.0 licence](#).

Any further distribution of this work must maintain attribution to the author(s) and the title of the work, journal citation and DOI.

Hao Kong¹ , Jintai Lin^{1,2,*} , Ruijing Ni³, Mingxi Du⁴, Jingxu Wang^{5,6} , Lulu Chen⁷, Chenghao Xu¹, Yingying Yan⁸, Hongjian Weng^{1,9} and Yuhang Zhang¹ ¹ Laboratory for Climate and Ocean-Atmosphere Studies, Department of Atmospheric and Oceanic Sciences, School of Physics, Peking University, Beijing 100871, People's Republic of China² Institute of Carbon Neutrality, Peking University, Beijing 100871, People's Republic of China³ Minerva Research Group, Max Planck Institute for Chemistry, Mainz 55128, Germany⁴ School of Public Policy and Administration, Xi'an Jiaotong University, Xi'an 710049, People's Republic of China⁵ Frontier Science Center for Deep Ocean Multispheres and Earth System (FDOMES) and Physical Oceanography Laboratory, Ocean University of China, Qingdao 266100, People's Republic of China⁶ College of Oceanic and Atmospheric Sciences, Ocean University of China, Qingdao 266100, People's Republic of China⁷ Department of Environmental and Occupational Health, Milken Institute School of Public Health, George Washington University, Washington, DC 20052, United States of America⁸ Department of Atmospheric Science, School of Environmental Sciences, China University of Geosciences, Wuhan 430074, People's Republic of China⁹ Now at China Satellite Network Application Co., Ltd, Beijing 100095, People's Republic of China

* Author to whom any correspondence should be addressed.

E-mail: linjt@pku.edu.cn**Keywords:** nitrogen oxides, emission, pollution control, city-level, satelliteSupplementary material for this article is available [online](#)**Abstract**

Nitrogen oxides ($\text{NO}_X = \text{NO} + \text{NO}_2$) are a major air pollutant under stringent emission regulation in China. The nation has effectively cut its total anthropogenic emission since the peaking around 2012, with cities at the forefront of implementing mitigation measures. However, the city-level emission changes and cross-city contrast remains poorly understood, due to inaccuracies in existing emission data. Using the satellite-based high-resolution PHLET inversion, we derived city-level NO_X emissions in China from 2012 to 2020. We found much weaker emission declines in small cities (by 14.7% from 2012–2014 mean to 2018–2020 mean, for the bottom one-third of cities ordered by economic volumes) and medium cities (by 21.3%, for the middle one-third), compared to those in large cities (by 30.6%, for the top one-third) and provincial capital cities in the North Region of China (by 54.2%). Emissions even grew in 43.0% of small cities, compared to 17.4% for large cities. Cross-city emission differences both within each province and among the provinces decreased substantially over time, resulting in a relative shift of emission burdens towards small and medium cities. Such a tendency is hardly resolved by bottom-up emission inventories, highlighting the value of satellite-based high-resolution inversion for tracking city-level emissions to support targeted emission control.

1. Introduction

Tropospheric nitrogen oxides ($\text{NO}_X = \text{NO} + \text{NO}_2$) are a major air pollutant contributing to the formation of aerosols and ozone and affecting human health and climate (Seinfeld and Pandis 2016). As one of the largest NO_X emitting countries (Martin *et al* 2003, Hoesly *et al* 2018, Nguyen *et al* 2022), China

has issued a series of measures to reinforce regulations on air pollutant emissions since 2013 (China's State Council 2013, Geng *et al* 2024), resulting in substantial reduction of its national total NO_X emission after the peaking year around 2012 (Li *et al* 2017, Zheng *et al* 2018). During this process, China's cities have been playing a key role in implementing emission mitigation measures, including the well-known

'One City One Policy' action (MEE 2021). Thus, it is crucial to understand how the city-level emissions have been changing over time and how the performance of emission mitigation has differed across cities, in order to support China's further targeted environmental strategies. Yet, such knowledge remains poor, primarily due to the lack of local information in constructing detailed city-level emission datasets.

Previous research on emission trends in China and their spatial disparity was focused on provincial and/or regional scales (Wu *et al* 2017, Li *et al* 2022), given the lack of accurate city-level emission information. The widely-used bottom-up emission inventories implement proxy-based (such as gross domestic product (GDP) and population density) downscaling from national or provincial levels to target grids (Li *et al* 2017, Zheng *et al* 2021a), and thus are inadequate to account for inter-city heterogeneity in emission trends. These inventories adopt technology-based emission factors (EFs) (Li *et al* 2017) often by aggregating information from different locations, in which process the spatial disparity of EFs such as inter-city difference is not or inadequately retained. As a result, these emission datasets might have missed considerable amounts of emission sources in less-known places (Kong *et al* 2022).

Meanwhile, ground-based air quality monitoring, although abundant at large cities, suffers from a lack of measurement sites and spatial representativeness in many economically small and medium cities across the country (Cooper *et al* 2022, Luo *et al* 2022), which could substantially impact the evaluation of regional pollution trends¹⁴. And the measured pollutant concentrations are complexly linked to city-level emissions through nonlinear chemistry and transport, rather than being simply proportional to the latter. In the meantime, satellite remote sensing provides independent pollution monitoring with high spatial resolution and coverage, allowing for emission estimates at very fine scales (Liu *et al* 2017, Beirle *et al* 2019, Kong *et al* 2022, Qin *et al* 2023) to enable city-level emission quantification.

Satellite remote sensing of tropospheric nitrogen dioxide (NO₂) vertical column densities (VCDs) has been proven useful in air pollution research, especially in less-developed regions where ground-based measurements are sparse or absent (Ding *et al* 2017, Cooper *et al* 2022, Kong *et al* 2023). Satellite-based studies have revealed important emission sources missing from the inventories (Kong *et al* 2022, Pan *et al* 2023, Qin *et al* 2023), which could substantially influence the city-level emission trends. Nevertheless, most satellite-based emission estimates to date are subject to low spatial resolution (i.e. ≥ 25 km) (Ding *et al* 2020, Jung *et al* 2022, Qu *et al* 2022), making it hard to track the small-scale changes of NO_x emissions and capture the contrast across cities. Given the

spatial mixture of emission sources (such as industry, power and transportation) and the highly nonlinear chemistry of NO_x in Chinese cities, it is challenging for point-source-based plume (Liu *et al* 2017) methods or lifetime-fixed divergence models (Beirle *et al* 2019) to obtain reliable emission estimates at high resolution (e.g. 5 km) with adequate spatial coverage (Liu *et al* 2017, Beirle *et al* 2021, Wang *et al* 2024). A reliable, fine-scale satellite-based emission inversion is needed to quantify city-level emissions and their trends.

Here we adopted the emission inversion algorithm based on the Peking University High-resolution Lifetime-Emission-Transport model (PHLET, Kong *et al* 2019, 2022) and its adjoint model to quantitatively estimate city-level NO_x emissions in China, based on satellite NO₂ VCD data from the ozone monitoring instrument (OMI). In this study, we calculated summer (June, July and August) mean NO_x emissions over mainland China at $0.05^\circ \times 0.05^\circ$ based on stripe-corrected POMINO-OMI v2.1 NO₂ VCD data (Lin *et al* 2014, 2015, Liu *et al* 2019, Zhang *et al* 2022) from 2012 to 2020. The emission inversion results were evaluated by using independent GEOS-Chem simulations and ground-based NO₂ concentration measurements from the Ministry of Ecology and Environment (MEE). Then, the inter-annual variations and trends of NO_x emissions in individual cities were examined to reveal the inter-city contrast and its temporal evolution, including comparisons with available socioeconomic data, ground-based measurements and bottom-up emission inventories.

2. Method

The OMI instrument is onboard the sun-synchronous Aura satellite launched in July 2004. It offers monitoring of tropospheric NO₂ VCDs with daily global coverage at the local equator crossing time around 13:30 (Levelt *et al* 2006, Boersma *et al* 2018). OMI has a higher spatial resolution than its predecessors with a nadir pixel size of about $13 \text{ km} \times 24 \text{ km}$ (Levelt *et al* 2006, de Graaf *et al* 2016). It has been widely used in environmental research, including NO_x emission estimates from the global scale (Miyazaki *et al* 2012) to individual point sources (Beirle *et al* 2011).

For the inversion of NO_x emissions, we used summertime (June, July, and August) tropospheric NO₂ VCD data from the POMINO-OMI v2.1 product (Lin *et al* 2014, 2015, Liu *et al* 2019; last access: 10 February 2023), which is available for 2012 and later years. In comparison with the KNMI official product (QA4ECV v1.1; Boersma *et al* 2018), POMINO-OMI explicitly accounts for the impacts of aerosols and surface reflectance anisotropy on NO₂ VCD retrieval, and adopts *a priori* vertical profiles of NO₂ at a

higher horizontal resolution (25 km versus 100 km) (Lin *et al* 2014, 2015, Liu *et al* 2019, Zhang *et al* 2022). As detailed in S1–S2 of supplementary material, we followed Kong *et al* (2022) to filter satellite pixels for ensuring data quality and designed a destriping scheme based on the empirical distribution of POMINO-OMI v2.1 NO₂ VCD data to substantially reduce the noises caused by abnormal heterogeneity across different viewing angles of OMI.

Then, we adopted PHLET and its adjoint model for emission inversion as detailed in S3 of supplementary material, with several adjustments to better account for data uncertainty and background NO₂ influences. PHLET accounts for the location-specific nonlinear lifetime-abundance relationship and horizontal transport in linking NO₂ VCDs to NO_x emissions (Kong *et al* 2019, 2022). At low computational costs, PHLET is able to estimate NO_x emissions at a high spatial resolution (0.05° × 0.05° or finer) over a large domain with high accuracy. To isolate anthropogenic contributions, emissions from soil (Weng *et al* 2020) and open fire (Giglio *et al* 2013) sources were subtracted from PHLET-derived total emissions (Kong *et al* 2019, 2022). To remove potential noises in the derived anthropogenic emission data, we also filtered out the emissions at locations where three proxies (including Tencent user location, Tencent 2021; nighttime light, Hsu *et al* 2015; and road network, Feng *et al* 2019) suggested few human activities (Kong *et al* 2022). Finally, to minimize the impacts of missing data and sampling uncertainties of satellite NO₂ VCDs, we calculated the three-year moving averages of NO_x emissions — for example, emission data for 2013* represent the average over 2012–2014. For analysis, the emissions are expressed in units of Ton a⁻¹ or kg a⁻¹, based on the NO₂ molecular weight (46 g mol⁻¹) and a conversion from summer to the whole year with a scaling factor of 365/92.

The PHLET-derived NO_x emission data were independently validated by simulations with GEOS-Chem (v12.9.3; IGCUC 2020). See S4 of supplementary material) and the MEE ground-based NO₂ concentration measurements. Compared with using the Multi-resolution Emission Inventory for China (MEIC) v1.4 inventory (Zheng *et al* 2014, Liu *et al* 2015) to drive GEOS-Chem simulations, the PHLET emissions led to better consistency between GEOS-Chem simulated and MEE measured NO₂ concentrations in most years, and substantially improved the model performance in the interannual changes of NO₂ (see S4 of supplementary material).

The PHLET-derived emission dataset contains all of the 368 cities (including city-level regions such as Beijing) in mainland China. We filtered out 80 cities for subsequent analysis as follows. First, we excluded 16 cities where the POMINO-OMI NO₂

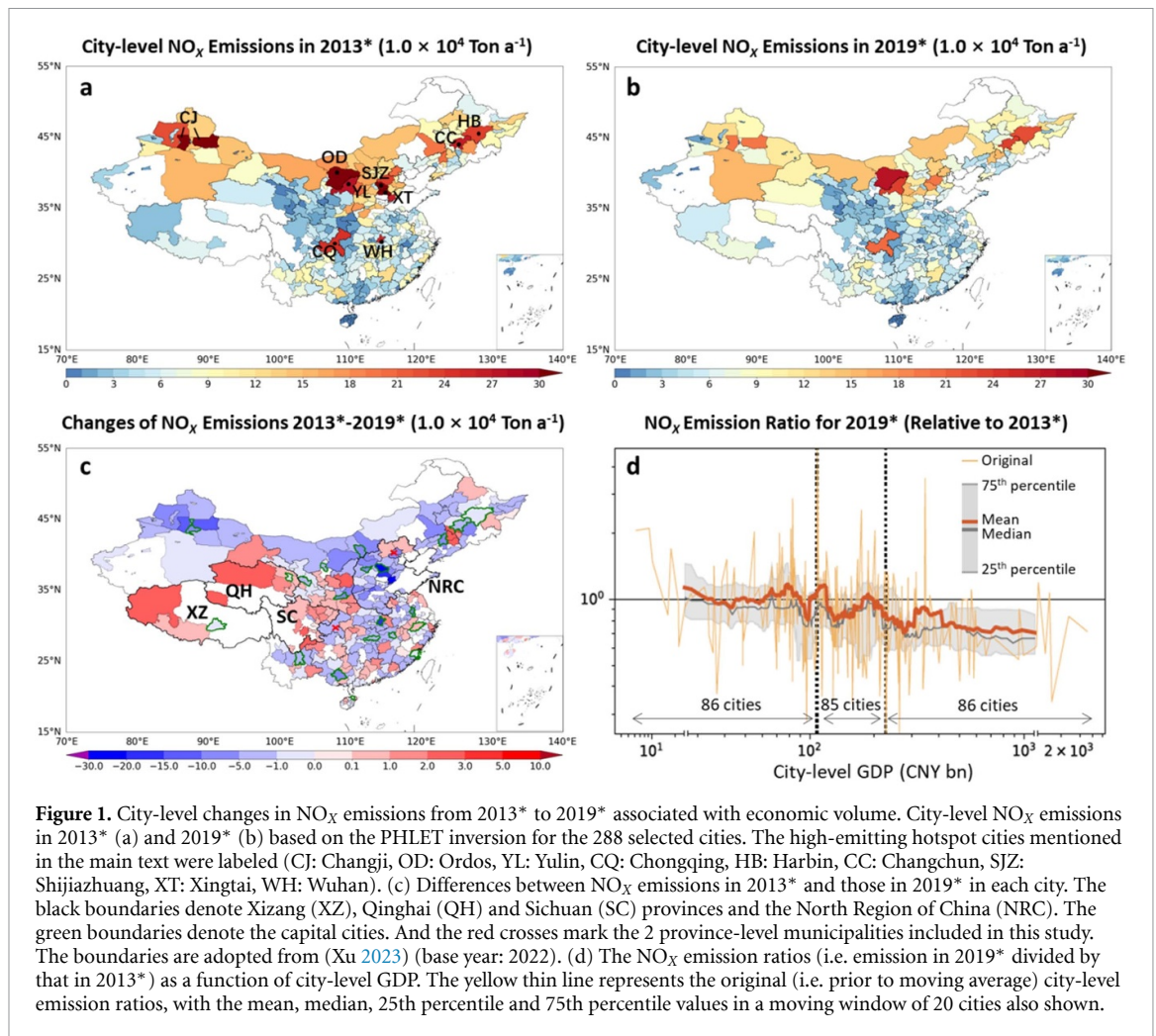
VCD data were insufficient to allow reliable inversion and 1 city where the inversion quality was substantially contaminated by steep topography (see S5 of supplementary material). After that, we compared the POMINO-OMI-based city-level emissions in 2019* with the respective emissions (Kong *et al* 2022) estimated based on the POMINO-TROPOMI v1.2 NO₂ VCD product (Liu *et al* 2020) for the Tropospheric Monitoring Instrument (TROPOMI, available since 2018). The POMINO-TROPOMI product has a higher spatial resolution and less noise such as stripes (Liu *et al* 2020). We then excluded 63 cities showing relatively large differences between OMI-based and TROPOMI-based emission inversions (see S5 of supplementary material). And NO_x emissions in the rest 288 cities showed reliable consistency ($R = 0.95$, $NMB = 0.0\%$, $P\text{-value} = 0.00$) between inversions based on POMINO-OMI and POMINO-TROPOMI NO₂ VCDs respectively. In all, we focused on the evolving trends of city-level NO_x emissions based on the 288 cities with the most reliable emission inversion, which contributed 77.5% of the anthropogenic emissions in the whole 368 cities in 2019*.

3. Results

3.1. Disparity in city-level NO_x emission changes

Our PHLET inversion shows that the total NO_x emission from the 288 cities decreased from $1.99 \pm 0.44 \times 10^7$ Ton a⁻¹ (with one standard deviation) in 2013* to $1.52 \pm 0.33 \times 10^7$ Ton a⁻¹ in 2019* (supplementary figure 9), with a relative decline by 24.0%. Despite the substantial emission reduction in the national level, major disparities in emission trends were found among the cities. As shown in figures 1(a)–(c), in 2013*, the NO_x emissions in the high-emitting cities (e.g. the cities labelled in figure 1(a)) were much higher than those in the surrounding cities. Yet by 2019*, such contrast was largely reduced, especially in the North Region of China (NRC) (NRC, the most polluted region in China). The top 50% of cities ranked by emission amounts contributed 81.9% of the 288-city total emission in 2013* but 98.9% of the total reduction from 2013* to 2019*. Moreover, the top-10 emitting cities contributed 14.9% of the total NO_x emission in 2013* but 24.9% of the overall reduction. Most cities (36 out of 38) in the NRC, 20 out of the 21 capital cities and two province-level municipalities showed decreasing NO_x emissions. By comparison, emission declines tended to be slower in the other cities, especially so in the western non-capital cities but also in the east. There were even a large proportion (20 out of 24) of western cities in Sichuan, Qinghai and Xizang (Tibet) provinces showing emission increases.

In general, high-emitting cities tended to cut off more NO_x emissions from 2013* to 2019*.

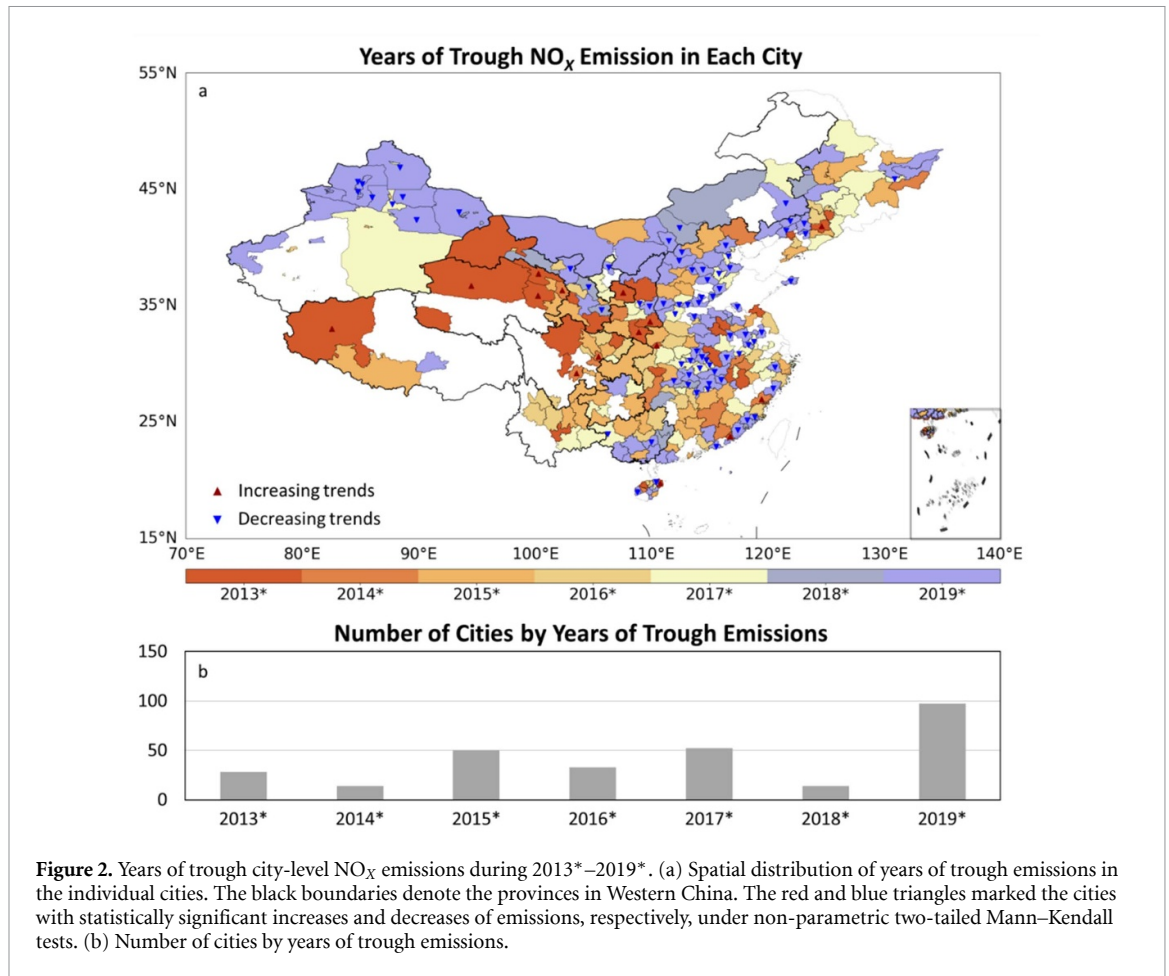


Thus, the contrast of emission amounts across cities was reduced substantially. For example, the contrast between NO_x emissions in Wuhan (labeled in figure 1(a)), the capital city of Hubei Province in Central China, and the average of its 7 neighboring cities was 3.43 ± 0.91 versus $0.60 \pm 0.15 \text{ kg km}^{-2} \text{ h}^{-1}$ in 2013* (around 5.7 times). By 2019*, the contrast decreased to 1.17 ± 0.29 versus $0.42 \pm 0.09 \text{ kg km}^{-2} \text{ h}^{-1}$ (around 2.8 times). NO_x emissions at the hotspot cities in the southern Hebei Province (Shijiazhuang and Xingtai cities, labeled in figure 1(a)) decreased notably by 59.5% (from $7.18 \pm 1.36 \times 10^5$ – $2.91 \pm 0.54 \times 10^5 \text{ Ton a}^{-1}$), far surpassing the average decrease of 41.4% in the NRC (from $48.3 \pm 10.7 \times 10^5$ to $28.3 \pm 5.1 \times 10^5 \text{ Ton a}^{-1}$) and 24.0% over mainland China.

The city-level emission trends were related to local economic status. Of the 288 cities, GDP data are available for 257 cities (CEIC 2022). We divided these 257 cities into three groups (small, medium, and large) based on their GDP in 2019, with a roughly equal number of cities in each group (figure 1(d)). For the 86 economically small cities (GDP < CNY 107.9 bn), NO_x emissions experienced a collective decline by 14.7% from 2013* to 2019*. Emissions

decreased in 49 cities but increased in 37 cities, with 18 cities showing substantial increases of more than 30%. These 86 cities contributed 26.0% of the 257-city total emission in 2019*, an increase from 23.2% in 2013*. Meanwhile, among the 85 medium cities (CNY 107.9 bn ≤ GDP < CNY 225.5 bn), emissions increased in 28 cities, with 11 cities experiencing increases of more than 30%. These 85 medium cities exhibited a collective emission decline by 21.3%. In contrast, among the 86 large cities (GDP ≥ CNY 225.5 bn), 71 experienced emission decreases, 15 experienced emission increases, and only 4 showed increases of more than 30%. Collectively, these 86 cities achieved an emission reduction by 30.6%, which was much more substantial than that for the small (14.7%) and medium (21.3%) cities. The large cities contributed 46.4% of the 257-city total emission in 2013*; however, this share decreased to 42.4% in 2019*.

Figure 1(d) further demonstrates that NO_x emissions tended to decrease proportionally more in cities with larger economic sizes denoted by GDP in 2019. To highlight the underlying relationship, the figure illustrates the variations of GDP values and NO_x emission ratios (i.e. emission in 2019* divided by that in 2013*)



after smoothing with a moving average of every 20 cities ordered by GDP. After moving average, the mean, median, 25th percentile and 75th percentile values of emission ratios show statistically significant negative correlations with GDP values ($R = -0.66, -0.68, -0.54, \text{ and } -0.61$, respectively, for emission ratio versus GDP). Similar GDP dependence of emissions is shown for individual years in supplementary figure 10.

Besides the modest declines in the economically small and medium cities in general, the city-level emissions experienced different pathways over the years. Figure 2 shows the year of trough (i.e. the lowest) NO_x emission in each city, and also marks emission decreases and rises with statistical significance (P -value < 0.05) under non-parametric two-tailed Mann–Kendall tests. Among the 288 cities, 75 experienced statistically significant decreases from 2013* to 2019*, 15 experienced statistically significant emission rises. A total of 163 cities experienced trough emissions after 2013* but before 2019*, and the trough emissions mostly occurred in 2015*–2017*, consistent with the variation of thermal power generation and coal consumptions (CEIC 2022) (supplementary figure 11). Specifically, thermal power generation in mainland China suspended its rising in 2015 (with a slight decrease of 0.3% from 2014), further

decreased by 11.5% from 2015 to 2016, and stayed at a relatively low level in 2017, despite the overall increasing trend by 3.2% per year from 2013 to 2019. Similarly, coal consumption in mainland China reached a low level in 2016. Particularly outside the NRC where the emission reduction targets (China, 2011, 2017) or emission control technology penetration (Tang *et al* 2020) were lower, the coal consumption decreased by 3.3% in 2015 from the previous year and remained low in 2016.

3.2. Emission contrasts within and across provinces

The cross-city disparity of NO_x emission changes led to a substantial alteration of emission distribution within each province, with increasing proportional contributions from the non-provincial-capital cities. Most of the provincial capital cities (17 out of 21 in this study, not including the province-level municipalities) cut off larger fractions of NO_x emissions than the non-capital cities within the same provinces did (figure 3). On average, NO_x emissions decreased by 37.7% (from $0.28 \pm 0.06 \times 10^7 \text{ Ton a}^{-1}$ to $0.18 \pm 0.04 \times 10^7 \text{ Ton a}^{-1}$) in capital cities, comparing to 21.7% (from $1.67 \pm 0.38 \times 10^7 \text{ Ton a}^{-1}$ to $1.30 \pm 0.29 \times 10^7 \text{ Ton a}^{-1}$) in non-capital cities during the years (table 1). Notably, the capital cities in

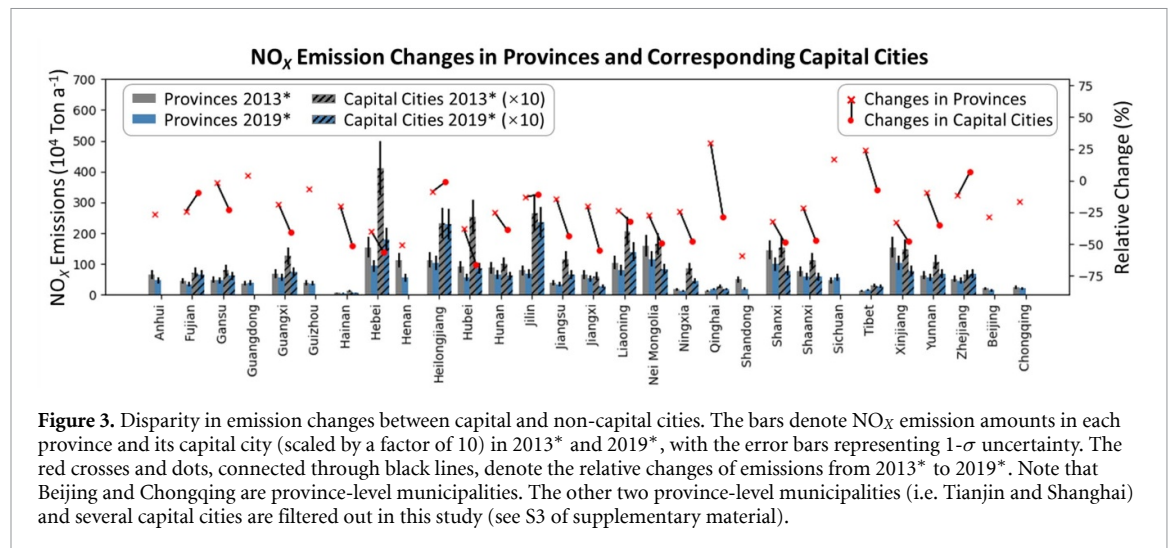


Figure 3. Disparity in emission changes between capital and non-capital cities. The bars denote NO_x emission amounts in each province and its capital city (scaled by a factor of 10) in 2013* and 2019*, with the error bars representing 1- σ uncertainty. The red crosses and dots, connected through black lines, denote the relative changes of emissions from 2013* to 2019*. Note that Beijing and Chongqing are province-level municipalities. The other two province-level municipalities (i.e. Tianjin and Shanghai) and several capital cities are filtered out in this study (see S3 of supplementary material).

Table 1. Changes of NO_x emission contrasts between capital and non-capital cities and between Eastern and Western China. Data are presented with 1-sigma uncertainties. An asterisk (*) next to a year indicates the center year of a 3-year moving average window (e.g. 2013* represents the average for 2012–2014). Results for capital cities do not include province-level municipalities (Beijing, Shanghai, Tianjin and Chongqing).

		Capital cities	Non-capital cities	Eastern China	Western China
Emission amount (10^7 Ton a^{-1})	2013*	0.28 ± 0.06	1.67 ± 0.38	1.27 ± 0.28	0.72 ± 0.18
	2019*	0.18 ± 0.04	1.30 ± 0.29	0.92 ± 0.18	0.60 ± 0.16
Emission per capita (kg a^{-1})	2013*	30.7 ± 6.4	16.9 ± 3.7	17.8 ± 3.9	20.0 ± 4.6
	2019*	18.5 ± 3.7	12.6 ± 2.7	12.4 ± 2.5	15.9 ± 3.9
Emission per unit GDP (g CNY^{-1})	2013*	0.35 ± 0.07	0.54 ± 0.12	0.41 ± 0.09	0.65 ± 0.16
	2019*	0.13 ± 0.03	0.29 ± 0.06	0.19 ± 0.04	0.35 ± 0.09

the NRC achieved a remarkable reduction of 54.2% on average.

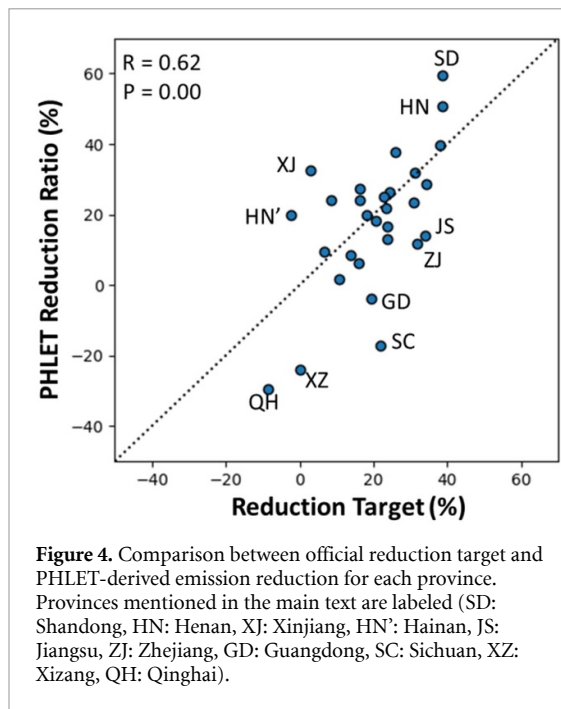
The relative contributions of emissions from capital cities to their provincial totals fell notably, especially in Western China (marked in figure 2, from 12.1% in 2013* to 8.6% in 2019*). This tendency of emission redistribution might be related in part to the faster urbanization rates in the non-capital cities (supplementary figure 12) — from 2013 to 2019, the urban population grew by 22.0% in the non-capital cities but 16.1% in the capital cities, with the contrast even greater in Western China (26.7% versus 8.5%).

As the contrast in NO_x emission amounts between capital and non-capital cities decreased, per capita emissions in both types of cities as well as their difference decreased substantially. As shown in table 1, in 2013*, the per capita emissions in capital cities were much higher than in non-capital cities (30.7 ± 6.6 versus $16.9 \pm 3.8 \text{ kg a}^{-1}$). From 2013* to 2019*, the average per capita emissions declined by 39.5% in capital cities, which was much greater than 25.1% in non-capital cities. By 2019*, the overall difference in per capita emissions between capital and non-capital cities became much smaller (18.5 ± 4.1 versus $12.6 \pm 2.8 \text{ kg a}^{-1}$). Such a reduction in emission contrast demonstrated the decentralizing tendency of regional environmental burdens, as a result

of how environmental policies were implemented within each province accompanied by potential inter-city migration of industry (Shen *et al* 2019).

Meanwhile, along with the faster economic growth in capital cities, the difference of NO_x emissions per unit GDP between capital and non-capital cities was further enlarged. As shown in table 1, the non-capital-to-capital ratio of NO_x emissions per unit GDP grew from 1.56 in 2013* (0.54 ± 0.12 versus $0.35 \pm 0.08 \text{ g CNY}^{-1}$) to 2.19 in 2019* (0.29 ± 0.06 versus $0.13 \pm 0.03 \text{ g CNY}^{-1}$). As the majority of capital cities (17 out of 21) had the highest GDP within their corresponding provinces, the increasing proportional difference of NO_x emissions per unit GDP was consistent with the abovementioned result that the economically larger cities tended to achieve greater emission reductions (figure 1(d)).

Besides the emission redistribution within each province, there were also notable inter-province differences in emission variations. Such results can be compared with the official province-level emission reduction targets in the 12th and 13th Five-Year Plans (State Council of the People's Republic of China 2011, 2017) (supplementary figure 13). Overall, the provinces in the east tended to have stricter reduction targets, especially in the NRC (figure 4). To focus on the comparison between the PHLET-derived and



targeted emission reductions at the province level, we summed up the PHLET-derived emission changes within each province (including the province-level municipalities).

The PHLET-derived province-level emission changes were in general agreement with the reduction targets, albeit with notable exceptions (figure 4). Thus, the national-level reduction target was achieved overall. At the provincial level, some exceptions were caused by our city filtering that removed much of the cities in some provinces. For example, had the 63 cities for which POMINO-OMI and POMINO-TROPOMI derived emissions exhibited larger differences (than allowed here) been included (supplementary figure 14), the provincial emission reductions would be changed from -3.8% (i.e. an increase) to 11.1% in Guangdong and from 14.1% to 33.2% in Jiangsu, which would be much closer to their respective emission reduction targets (19.4% in Guangdong, and 34.0% in Jiangsu).

Major gaps still existed in some of the provinces after accounting for the impacts of city filtering. Specifically, Xinjiang, Hainan, Shandong, and Henan provinces experienced much larger emission reductions than their targets. Among them, Xinjiang in Western China and Hainan in Southern China, albeit with low reduction targets (3.0% and -2.3% , respectively), also achieved substantial emission reductions (32.7% and 19.9% , respectively) based on PHLET, as a result of their tough measures to phase out outdated industrial capacity (Geng *et al* 2016, Li 2016).

In Shandong Province, where only four out of the 16 cities remained after city filtering, the

PHLET-derived emission reduction (59.3%) notably surpassed the target (38.8%). And such a difference remained (54.1% versus 38.8%) after including the other 12 cities which were filter out based on the comparison between POMINO-OMI and POMINO-TROPOMI derived emissions. The considerable emission reduction shown in PHLET emissions was likely attributed to strict environmental regulations to (more than) achieve the most ambitious reduction target among all provinces. Similarly, Henan Province, which had the second highest target (38.6%), also achieved a much higher emission reduction (50.7%) than the target. Together with Shandong, 18 cities in the two provinces achieved collective emission reduction of 53.3% , contributing to 18.0% of the total reduction in the 288 cities. Strict targets were also set in other provinces of the NRC to combat the heavy pollution (supplementary figure 13). Total NO_x emissions in the NRC decreased by 41.4% , contributing 41.8% of the total reduction in China.

On the contrary, the PHLET-derived emission reductions were much smaller than their respective targets in Sichuan and Xizang (-17.0% versus 21.8% in Sichuan, and -24.0% versus 0.0% in Xizang); and the PHLET-derived emission increases in Qinghai were much larger than its allowed growth (29.6% versus 8.4%) (figure 4). These undesirable emission trends were driven by the increases in most non-capital cities in Sichuan and all non-capital cities in Xizang and Qinghai (figures 1(a)–(c)). As a result, the relative contribution of these provinces together to the national emission total became larger over time.

In Zhejiang, the provincial emissions declined only slightly (by 11.8%), much smaller than its reduction target (31.9%). This result was caused by the slight increase in its capital city (Hangzhou) partly compensating the overall decline in its non-capital cities, consistent with the faster population growth in Hangzhou than Zhejiang's provincial average (12.6% versus 4.4%). Such a contrast in emission changes between Zhejiang's capital and non-capital cities is to the opposite direction of the contrast for most provinces.

3.3. Increasing contribution of emissions in western cities

The unequal changes in city-level NO_x emissions led to a reduction of emission contrast between the western and eastern cities. From 2013* to 2019*, the proportion of NO_x emissions from the western cities to the national total grew from 36.4% to 39.6% . Particularly, the total emission in the NRC in the east was 6.5 times the sum of emissions from Xizang, Qinghai and Sichuan in the west in 2013* but only 3.2 times in 2019*. Such a large-scale spatial redistribution of emissions was consistent with

the westward industrial migration (Li *et al* 2022) and increased economic production in the west to supply the national demand. As derived from multi-regional input–output tables (Wang *et al* 2019, Zheng *et al* 2020) (supplementary figure 15), industrial production of Western China to supply demands from the provinces outside (inside) Western China grew by 45.0% (34.0%) from 2012 to 2017; and the growth rate of gross output in the west far exceeded the other provinces (42.0% versus 30.0%).

The weakening of contrast between high- and low-emitting cities was less remarkable in Western China than in the east. Over the years, NO_x emissions in the top 10% (17 out of 174) and the first half of high-emitting cities (ranked by emissions in 2013*) in the east decreased by 41.7% and 31.6%, respectively. By comparison, NO_x emissions in the top 10% (11 out of 114) and the first half of high-emitting cities in Western China decreased by only 29.0% and 21.8%, respectively. In Western China, NO_x emissions were more concentrated in the high-emitting cities, as the top 10% high-emitting cities contributed 34.1% of the total emission (in Western China) in 2013* and 29.3% in 2019*. In the east, however, the respective ratio was smaller and underwent a larger decline, at 29.4% in 2013* and 23.8% in 2019*. Thus, between 2013* and 2019*, most of the emission hotspot cities in Eastern China became much less notable (except around Changchun and Harbin in the northeast), but the hotspots in the western cities remained conspicuous, including Ordos, Yulin, Chongqing, and Changji (figures 1(a) and (b)).

Furthermore, although both Western and Eastern China experienced reductions of per capita emission over time (table 1), the pace of reduction in the west lagged behind. In 2013*, the average per capita NO_x emission in the west surpassed that in the east by 12.4% (20.0 ± 4.6 versus 17.8 ± 3.9 kg a⁻¹). And such difference further increased to 28.2% (15.9 ± 3.9 versus 12.4 ± 2.5 kg a⁻¹) in 2019*. Similarly, the relative west-to-east difference in NO_x emissions per unit GDP also became larger, from 58.5% (0.65 ± 0.16 versus 0.41 ± 0.09 g CNY⁻¹) in 2013*, to 84.2% (0.35 ± 0.09 versus 0.19 ± 0.04 g CNY⁻¹) in 2019*. This is in contrast to that the GDP in the east kept higher than in the west (by 198.8% in 2013 and 193.3% in 2019 for the 257 cities with available GDP data).

Overall, the rapid changes in west-to-east contrast within only a few years highlight the considerable inter-regional disparity in emission trends, as driven by the geographical changes in economic structure (Wu *et al* 2017, Li *et al* 2022) and inter-regional differences in emission control policy (China's State Council State 2011, 2017) and technology (Tang *et al* 2020). The evolving contrasts of emissions and economies reflected the emerging challenges to

balance development and environment in economically small and medium cities, which were typically non-capital and in the west.

3.4. Consistency with surface NO₂ measurements

The temporally evolving emission contrasts between Western and Eastern China, and between capital and non-capital cities based on our inversion were broadly consistent with the changes in summertime surface NO₂ concentrations from MEE ground-based measurements. As shown in supplementary figure 16(a), from 2013 to 2019, the average measured NO₂ concentrations in Eastern China were similar to or slightly higher than those in the west in the early years, and then became much lower than the latter in later years. Such an evolving contrast of NO₂ concentrations was consistent with our finding of higher emission amounts in the eastern cities and the decreasing east-to-west difference. Similarly, although the average NO₂ concentration in all capital cities kept higher than that in the non-capital cities in all years, their difference was declining over time (supplementary figure 16(b)), consistent with the within-province redistribution of city-level emissions.

There were four provinces with the PHLET-derived emission reductions being substantially lower than their officially-set reduction targets, including Xizang, Qinghai, Sichuan and Zhejiang. The MEE measurement data showed that 33 sites (or 64.7%) in the non-capital cities of Xizang, Qinghai and Sichuan showed increasing NO₂ concentrations from 2015 to 2019 (the data filtering described in S6 of supplementary material); note that no MEE site was set before 2015 in 16 out of 22 cities in this study. In Zhejiang, the average NO₂ concentration in summer declined notably, in contrast to the small anthropogenic emission reduction derived here. This contrast is because although the reduction of anthropogenic NO_x emissions was minor in Zhejiang, its emissions from open fire decreased by 85.2% (and by 87.3% in Hangzhou, its capital city) according to the GFED dataset (v4.1, last access: 08 December 2022; Giglio *et al* 2013). Based on our inversion, the overall (anthropogenic + open fire + soil) emissions decreased by 30.4% (by 27.2% in Hangzhou) from 2013* to 2019*. Note that open fire emissions might include emissions from straw burning as a result of agricultural activity, which however was not characterized as anthropogenic (fossil fuel + biofuel) here following the convention in emission inventories.

Compared to the spatial coverage by POMINO-OMI NO₂ VCDs and PHLET NO_x emissions, the coverage of ground-based MEE sites was inadequate to fully track city-level emission changes, especially in the non-capital cities whose fractional emission contributions had become increasingly important. By

June 2014, MEE sites had been established in all capital cities and province-level municipalities, but only in 91 non-capital cities (or 34.3%). By June 2019, no MEE sites were established in 27 non-capital cities. On average, there were about 10 sites in each capital city by June 2019, comparing to only four sites in each non-capital city. The lack of MEE sites was particularly notable in the economically small and medium cities, which was also a reflection of less stringent environmental regulations in these cities (Zhao *et al* 2024). Up to June 2019, on average, these small and medium cities had one monitoring site per 11 300 km² and per 5300 km² of area, respectively, compared to one site per 2500 km² in the other cities. Given the slower emission declines or even rises in these cities, substantially enhancing the coverage of ground-based monitoring in these cities, together with continuous high-resolution satellite measurements, would be particularly valuable to support timely, targeted emission control.

3.5. Differences from bottom-up inventories

The PHLET-derived inter-city contrast in NO_x emission trends is much larger than those shown in current bottom-up inventories. Here we evaluated three widely-used inventories, including MEIC (MEIC v1.4, last access: 04 August 2023; Zheng *et al* 2014, Liu *et al* 2015), Emissions Database for Global Atmospheric Research (EDGAR v8.1, last access: 10 June 2024; Crippa *et al* 2020) and Community Emissions Data System (CEDS v2021-04-21, last access: 09 August 2021; Hoesly *et al* 2018). As shown in supplementary figure 17, the three inventories suggested a relatively spatially-homogeneous emission trend over large areas, with overall decreases in all but 18, 14, and 4 cities, respectively, during the years. In consequence, the contrast in emission amounts between high- and low-emitting cities varied little or even increased over time in the inventories. These inventories suggested temporally stable emission contrasts between capital and non-capital cities and between western and eastern cities (supplementary table 2), with year-to-year fluctuations of cross-city contrasts being within $\pm 0.5\%$ and $\pm 1.5\%$, respectively. In addition, the correlation between the provincial-level emission changes in the inventories and the official reduction targets was much weaker than the correlation between PHLET-derived emission reductions and the targets (0.62 in figure 4 versus 0.28, 0.53, and 0.42 in supplementary figures 18(a)–(c)); this result is robust to our city filtering (supplementary figures 14 and 18(d)–(f)).

The weak city-level NO_x emission contrasts in the inventories could be attributed to errors in EFs, economic activity data, and downscaling approaches attributing provincial emission totals to individual locations (Geng *et al* 2017, Li *et al* 2017). As such, there might be considerable amounts of emission

sources missing from the inventories (Kong *et al* 2022). Such limitations could become even severer for more recent years, due to outdated/absent local information (such as road network and industries) in the inventories. In fact, over the years, the cross-city correlation of emissions between our inversion and these inventories weakened (supplementary figure 19(a)), and the difference in emission amounts in Western China between our inversion and these inventories increased (supplementary figure 19(b)).

4. Discussion

Our results about the evolving contrasts of city-level emissions were robust to the inversion uncertainties. Such uncertainties were attributed to the imperfect PHLET algorithm, POMINO-OMI satellite NO₂ VCDs and subtraction of open fire + soil emissions. By considering the effects of atmospheric transport and non-linear chemistry of NO_x, and improving the satellite NO₂ VCDs with effective de-striping, the impacts of inversion uncertainties on the derived city-level emission contrasts were limited. And excluding cities in which the emission inversion in 2019* based on POMINO-OMI NO₂ VCDs showed relatively large deviations from that based on POMINO-TROPOMI NO₂ VCDs further reduced the impact of inversion uncertainties (see S3 of supplementary material). Moreover, our results were robust to the city filtering — examining the 351 cities with no TROPOMI-based city filtering would show similar cross-city emission contrast (supplementary figures 20–21 & supplementary table 3). From 2016 to 2017 and from 2018 to 2019, there existed notable reductions of open fire emissions in Eastern China; and combining anthropogenic and open fire emissions (i.e. only soil emissions were removed) would further augment the cross-city contrast in emission trends. Our emission inversion was conducted for summer, but the impact of emission seasonality on emission trends was insignificant — as indicated by the bottom-up inventories, the trends of summertime emissions were highly consistent with the trends of annual emissions (supplementary figure 9). Although the last year of our emission inversion, 2020, experienced the breakout of COVID-19 pandemic in 2019/2020 winter, the emissions after May 2020 had returned to the level in 2019 over mainland China (Zheng *et al* 2021b, supplementary figure 7); and our derived summertime emission changes from 2018* to 2019* were consistent with the overall tendencies (e.g. supplementary figure 9). A sensitivity test excluding the emission (see S7 of supplementary material) in 2020 also indicated little impact on our results.

We also examined the potential relationships between relative changes in NO_x emissions and multiply socioeconomic indicators, including total GDP, GDP of the secondary industry, population and

vehicle ownerships. We found that cities with stronger relative growth in total GDP and GDP of the secondary industry tended to have experienced weaker relative emission reduction ($R = 0.12\text{--}0.13$, see S8 of supplementary material). As economic growth remains a central task of China, especially for many small and medium cities, such correlations highlighted the difficulties in reconciling economic growth with emission control.

Overall, our study showed the capability of satellite-based high-resolution emission inversion to track emission changes at the city level over a large domain like mainland China, which remains a very difficult task for bottom-up emission inventories given their lack of local information in constructing the emission datasets. Our inversion revealed relatively weak declines of anthropogenic emissions in economically small (by 14.7%) and medium (by 21.3%) cities during 2013*–2019*. The relative emission reduction in these cities was smaller than that of the total anthropogenic emission of mainland China (by 24.0%). And it shows sharp contrast to the much more substantial decreases in economically large cities (by 30.6%, most of which are highly emitting and located in Eastern China), particularly capital cities in the NRC (by 54.2%). Emissions grew in 43.0% of small cities and 32.9% of medium cities, compared to only 17.4% for large cities. The inter-city disparity in emission changes led to notable redistribution of emissions from capital to non-capital cities within each province, and from Eastern to Western China, with several provinces (mostly in the west) failing to meet their emission reduction targets. Such emission contrast and redistribution might have led to far-reaching environmental impacts via atmospheric transport and nonlinear chemistry, such as the formation of ozone and particulate matter. It raises new challenges for future environmental management and economic development strategy to allow sustainable city development, especially in many less-known small or medium cities across the country.

As many of the small and medium cities suffer from no or insufficient ground-based air pollution measurement sites, enhancing the monitoring network would be an effective immediate step to improve environmental management, for example, by establishing and maintaining necessary amounts of measurement sites. To this end, high-quality satellite-based remote sensing and emission inversion, as demonstrated here, will continue to provide invaluable independent information to monitor and assess local air pollution and emissions.

Data availability statement

The data that support the findings of this study are openly available at the following URL/DOI: <https://www.pku-atmos-acm.org/acmProduct>. Data will be available from 1 August 2025.

Acknowledgments

This research is supported by the National Natural Science Foundation of China (Grant No. 42430603), the National Key Research and Development Program of China (Grant No. 2023YFC3705802), the National Natural Science Foundation of China (Grant No. 42075175), and the China Postdoctoral Science Foundation (Grant No. 2024M760087). We thank for the technical support of the National Large Scientific and Technological Infrastructure “Earth System Numerical Simulation Facility” (<https://cstr.cn/31134.02.EL>). Jingxu Wang is supported by the National Natural Science Foundation of China (Grant No. 42405186). We thank Yiwen Hu for help to evaluate the emission inversion.

ORCID iDs

Hao Kong  <https://orcid.org/0000-0001-5038-2914>

Jintai Lin  <https://orcid.org/0000-0002-2362-2940>

Jingxu Wang  <https://orcid.org/0000-0002-5642-9880>

Hongjian Weng  <https://orcid.org/0000-0003-1886-9452>

Yuhang Zhang  <https://orcid.org/0000-0001-9027-845X>

References

- Beirle S, Boersma K F, Platt U, Lawrence M G and Wagner T 2011 Megacity emissions and lifetimes of nitrogen oxides probed from space *Science* **333** 1737–9
- Beirle S, Borger C, Dörner S, Eskes H, Kumar V, de Laat A and Wagner T 2021 Catalog of NO_x emissions from point sources as derived from the divergence of the NO₂ flux for TROPOMI *Earth Syst. Sci. Data* **13** 2995–3012
- Beirle S, Borger C, Dörner S, Li A, Hu Z, Liu F, Wang Y and Wagner T 2019 Pinpointing nitrogen oxide emissions from space *Sci. Adv.* **5** eaax9800
- Boersma K *et al* 2018 Improving algorithms and uncertainty estimates for satellite NO₂ retrievals: results from the quality assurance for essential climate variables (QA4ECV) project *Atmos. Meas. Tech.* **11** 6651–78
- CEIC 2022 China premium dataset
- Cooper M J, Martin R V, Hammer M S, Levelt P F, Veeffkind P, Lamsal L N, Krotkov N A, Brook J R and McLinden C A 2022 Global fine-scale changes in ambient NO₂ during COVID-19 lockdowns *Nature* **601** 380–7
- Crippa M, Solazzo E, Huang G, Guizzardi D, Koffi E, Muntean M, Schieberle C, Friedrich R and Janssens-Maenhout G 2020 High resolution temporal profiles in the emissions database for global atmospheric research *Sci. Data* **7** 121
- de Graaf M, Sihler H, Tilstra L G and Stammes P 2016 How big is an OMI pixel? *Atmos. Meas. Tech.* **9** 3607–18
- Ding J, van der A R J, Eskes H J, Mijling B, Stavrou T, van Geffen J H G M and Veeffkind J P 2020 NO_x emissions reduction and rebound in China due to the COVID-19 crisis *Geophys. Res. Lett.* **47** e2020GL089912
- Ding J, van der A R J, Mijling B and Levelt P F 2017 Space-based NO_x emission estimates over remote regions improved in DECSO *Atmos. Meas. Tech.* **10** 925–38
- Feng X, Xiu C, Bai L and Wen Y 2019 Urban centrality and influencing factors in Jilin Province from the perspective of highway traffic flow *Econ. Geogr.* **39** 64–72

- Geng G *et al* 2024 Efficacy of China's clean air actions to tackle PM_{2.5} pollution between 2013 and 2020 *Nat. Geosci.* **17** 987–94
- Geng G, Zhang Q, Martin R V, Lin J, Huo H, Zheng B, Wang S and He K 2017 Impact of spatial proxies on the representation of bottom-up emission inventories: a satellite-based analysis *Atmos. Chem. Phys.* **17** 4131–45
- Geng J, Ren B, Lv Y-L and Wang T-Y 2016 Estimation of Co-benefits from pollution emission reduction by eliminating backward production capacities in Hainan Province *Environ. Sci.* **37** 2401–8
- Giglio L, Randerson J T and van der Werf G R 2013 Analysis of daily, monthly, and annual burned area using the fourth-generation global fire emissions database (GFED4) *J. Geophys. Res.* **118** 317–28
- Hoesly R *et al* 2018 Historical (1750–2014) anthropogenic emissions of reactive gases and aerosols from the community emissions data system (CEDS) *Geosci. Model Dev.* **11** 369–408
- Hsu F-C, Baugh K E, Ghosh T, Zhizhin M and Elvidge C D 2015 DMSP-OLS radiance calibrated nighttime lights time series with intercalibration *Remote Sens.* **7** 1855–76
- The International GEOS-Chem User Community 2020 geoschem/geos-chem: GEOS-Chem 12.9.3. The international GEOS-chem user community (<https://doi.org/10.5281/zenodo.3974569>) (Accessed 21 February 2021)
- Jung J, Choi Y, Mousavinezhad S, Kang D, Park J, Pouyaei A, Ghahremanloo M, Momeni M and Kim H 2022 Changes in the ozone chemical regime over the contiguous United States inferred by the inversion of NO_x and VOC emissions using satellite observation *Atmos. Res.* **270** 106076
- Kong H, Lin J, Chen L, Zhang Y, Yan Y, Liu M, Ni R, Liu Z and Weng H 2022 Considerable unaccounted local sources of NO_x emissions in China revealed from satellite *Environ. Sci. Technol.* **56** 7131–42
- Kong H, Lin J, Zhang R, Liu M, Weng H, Ni R, Chen L, Wang J, Yan Y and Zhang Q 2019 High-resolution (0.05° × 0.05°) NO_x emissions in the Yangtze River Delta inferred from OMI *Atmos. Chem. Phys.* **19** 12835–56
- Kong H, Lin J, Zhang Y, Li C, Xu C, Shen L, Liu X, Yang K, Su H and Xu W 2023 High natural nitric oxide emissions from lakes on Tibetan Plateau under rapid warming *Nat. Geosci.* **16** 474–7
- Levelt P F, van den Oord G H J, Dobber M R, Malkki A, Visser H, de Vries J, Stammes P, Lundell J O V and Saari H 2006 The ozone monitoring instrument *IEEE Trans. Geosci. Remote Sens.* **44** 1093–101
- Li M *et al* 2017 Anthropogenic emission inventories in China: a review *Natl Sci. Rev.* **4** 834–66
- Li M, Li Q, Wang Y and Chen W 2022 Spatial path and determinants of carbon transfer in the process of inter provincial industrial transfer in China *Environ. Impact Assess. Rev.* **95** 106810
- Lin J T, Liu M Y, Xin J Y, Boersma K F, Spurr R, Martin R and Zhang Q 2015 Influence of aerosols and surface reflectance on satellite NO₂ retrieval: seasonal and spatial characteristics and implications for NO_x emission constraints *Atmos. Chem. Phys.* **15** 11217–41
- Lin J T, Martin R V, Boersma K F, Sneep M, Stammes P, Spurr R, Wang P, Van Roozendaal M, Clémer K and Irie H 2014 Retrieving tropospheric nitrogen dioxide from the ozone monitoring instrument: effects of aerosols, surface reflectance anisotropy, and vertical profile of nitrogen dioxide *Atmos. Chem. Phys.* **14** 1441–61
- Liu F, Beirle S, Zhang Q, van der A R J, Zheng B, Tong D and He K 2017 NO_x emission trends over Chinese cities estimated from OMI observations during 2005–2015 *Atmos. Chem. Phys.* **17** 9261–75
- Liu F, Zhang Q, Tong D, Zheng B, Li M, Huo H and He K B 2015 High-resolution inventory of technologies, activities, and emissions of coal-fired power plants in China from 1990 to 2010 *Atmos. Chem. Phys.* **15** 13299–317
- Liu M *et al* 2019 Improved aerosol correction for OMI tropospheric NO₂ retrieval over East Asia: constraint from CALIOP aerosol vertical profile *Atmos. Meas. Tech.* **12** 1–21
- Liu M *et al* 2020 A new TROPOMI product for tropospheric NO₂ columns over East Asia with explicit aerosol corrections *Atmos. Meas. Tech.* **13** 4247–59
- Luo H *et al* 2022 The impact of the numbers of monitoring stations on the national and regional air quality assessment in China during 2013–18 *Adv. Atmos. Sci.* **39** 1709–20
- Martin R V, Jacob D J, Chance K, Kurosu T P, Palmer P I and Evans M J 2003 Global inventory of nitrogen oxide emissions constrained by space-based observations of NO₂ columns *J. Geophys. Res.* **108** 4537
- Ministry of Ecology and Environmental of the People's Republic of China 2021 Work plan for tracking the coordinated control of fine particulate matter and ozone pollution with 'one city, one policy' approach (available at: https://www.mee.gov.cn/xxgk2018/xxgk/xxgk04/202104/t20210428_831139.html) (Accessed 2 January 2025)
- Miyazaki K, Eskes H J and Sudo K 2012 Global NO_x emission estimates derived from an assimilation of OMI tropospheric NO₂ columns *Atmos. Chem. Phys.* **12** 2263–88
- Nguyen D-H, Lin C, Vu C-T, Cheruiyot N K, Nguyen M K, Le T H, Lukkhasorn W, Vo T D H and Bui X-T 2022 Tropospheric ozone and NO_x: a review of worldwide variation and meteorological influences *Environ. Technol. Innov.* **28** 102809
- Pan Y *et al* 2023 Widespread missing super-emitters of nitrogen oxides across China inferred from year-round satellite observations *Sci. Total Environ.* **864** 161157
- Qin K, Lu L, Liu J, He Q, Shi J, Deng W, Wang S and Cohen J B 2023 Model-free daily inversion of NO_x emissions using TROPOMI (MCMFE-NO_x) and its uncertainty: declining regulated emissions and growth of new sources *Remote Sens. Environ.* **295** 113720
- Qu Z, Henze D K, Worden H M, Jiang Z, Gaubert B, Theys N and Wang W 2022 Sector-based top-down estimates of NO_x, SO₂, and CO emissions in East Asia *Geophys. Res. Lett.* **49** e2021GL096009
- Seinfeld J H and Pandis S N 2016 *Atmospheric Chemistry and Physics: From Air Pollution to Climate Change* (Wiley)
- Shen J, Wang S, Liu W and Chu J 2019 Does migration of pollution-intensive industries impact environmental efficiency? Evidence supporting "pollution haven hypothesis" *J. Environ. Manage.* **242** 142–52
- State Council of the People's Republic of China 2011 CHINA: 12th Five-Year Plan for Energy Saving and Emission Reduction (available at: https://www.gov.cn/gongbao/content/2011/content_1947196.htm) (Accessed 24 May 2024)
- State Council of the People's Republic of China 2013 The Action Plan for Air Pollution Prevention and Control (available at: https://www.gov.cn/gongbao/content/2013/content_2496394.htm) (Accessed 24 May 2024)
- State Council of the People's Republic of China 2017 CHINA: 13th Five-Year Plan for Energy Saving and Emission Reduction (available at: https://www.gov.cn/gongbao/content/2017/content_5163448.htm) (Accessed 24 May 2024)
- Tang L, Xue X, Qu J, Mi Z, Bo X, Chang X, Wang S, Li S, Cui W and Dong G 2020 Air pollution emissions from Chinese power plants based on the continuous emission monitoring systems network *Sci. Data* **7** 325
- Tencent 2021 Tencent location big data (available at: <https://xingyun.map.qq.com/index.html>) (Accessed 2 September 2021)
- Li W-G 2016 Effects analysis of Xinjiang main pollutant total amount control during the "12th five-year plan period" *Arid Environ. Monit.* **30** 142–4
- Wang J *et al* 2019 Environmental taxation and regional inequality in China *Sci. Bull.* **64** 1691–9
- Wang S, Lin J, Kong H, Zhang Y, Xu C, Li C and Ren F 2024 Comparison of satellite-based fast inversion methods for nitrogen oxides emissions *Adv. Earth Sci.* **39** 269–78

- Weng H, Lin J, Martin R, Millet D B, Jaeglé L, Ridley D, Keller C, Li C, Du M and Meng J 2020 Global high-resolution emissions of soil NO_x, sea salt aerosols, and biogenic volatile organic compounds *Sci. Data* **7** 148
- Wu H, Guo H, Zhang B and Bu M 2017 Westward movement of new polluting firms in China: pollution reduction mandates and location choice *J. Comp. Econ.* **45** 119–38
- Xu X 2023 Multi-year city-level administrative boundary data of China *Resource and Environmental Science Data Platform* (<https://doi.org/10.12078/2023010102>)
- Zhang Y, Lin J, Liu M, Kong H, Chen L, Weng H and Li C 2022 High-resolution tropospheric NO₂ retrieval over Asia based on OMI POMINO v2.1 and quantitative comparison with other products *Nat'l Remote Sens. Bull.* **26** 971–87
- Zhao J, Tang Y, Zhu X and Zhu J 2024 National environmental monitoring and local enforcement strategies *Nat. Cities* **2** 58–69
- Zheng B et al 2018 Trends in China's anthropogenic emissions since 2010 as the consequence of clean air actions *Atmos. Chem. Phys.* **18** 14095–111
- Zheng B, Cheng J, Geng G, Wang X, Li M, Shi Q, Qi J, Lei Y, Zhang Q and He K 2021a Mapping anthropogenic emissions in China at 1 km spatial resolution and its application in air quality modeling *Sci. Bull.* **66** 612–20
- Zheng B, Huo H, Zhang Q, Yao Z L, Wang X T, Yang X F, Liu H and He K B 2014 High-resolution mapping of vehicle emissions in China in 2008 *Atmos. Chem. Phys.* **14** 9787–805
- Zheng B, Zhang Q, Geng G, Chen C, Shi Q, Cui M, Lei Y and He K 2021b Changes in China's anthropogenic emissions and air quality during the COVID-19 pandemic in 2020 *Earth Syst. Sci. Data* **13** 2895–907
- Zheng H, Zhang Z, Wei W, Song M, Dietzenbacher E, Wang X, Meng J, Shan Y, Ou J and Guan D 2020 Regional determinants of China's consumption-based emissions in the economic transition *Environ. Res. Lett.* **15** 074001